# Electronic structures of ordered Ag-Mg alloys

Yan Liu, R.G. Jordan, and S.L. Qiu
*Alloy Research Center, Department of Physics, Florida Atlantic University, Boca Raton, Florida 33431*
(Received 17 September 1993; revised manuscript received 2 November 1993)

We have investigated the electronic structures of the valence bands of $\beta'$-AgMg (CsCl structure) and $\alpha'$-$Ag_3Mg$ ($DO_{23}$ structure) by a combination of ultraviolet and x-ray photoelectron spectroscopies and first-principles band-structure and photocurrent calculations. The overall agreement between the measurements and calculated results is good indicating that the one-electron approach provides a realistic description of the electronic structure in Ag-Mg ordered alloys. We also present results for the core-level shifts observed on alloying.

## I. INTRODUCTION

The physical and metallurgical properties of alloys, such as their conductivity, structure, phase stability, etc., depend on the underlying electronic structure. Thus the principal requirement for any theory of alloys that is to lead to a detailed understanding of such properties is that it has to provide an accurate description of the electronic structure. It is essential therefore that the validity of the results of any calculational scheme should be adequately examined by the use of suitable experimental techniques. It is now generally accepted that photoelectron spectroscopy is the most sensitive and useful experimental probe of the surface and bulk electronic structure in metallic alloys.[1] By using this technique together with the appropriate first-principles theoretical calculational schemes therefore, it should be possible to gain key new insights into the electronic origin of many of the interesting and complex properties of metallic alloys. Here we present a study of the electronic structures of two ordered Ag-Mg alloys, namely, $\beta'$-AgMg and $\alpha'$-$Ag_3Mg$, through a combination of photoelectron spectroscopy and first-principles band-structure and photocurrent calculations. $\beta'$-AgMg has the CsCl structure and it remains ordered to its melting point.[2,3] It has an electron/atom ($e/a$) ratio of 3/2 and is a member of a special class of alloys commonly referred to as Hume-Rothery phases (or electron compounds) whose structures are strongly correlated with the $e/a$ ratio.[4] Ag-Mg alloys around the 3:1 stoichiometric composition undergo a transformation on cooling at about 390 °C (for 24% Mg) from a disordered fcc phase to a one-dimensional long period superlattice (LPS) structure.[2,3,5] One-dimensional LPS's are not uncommon; they exist in a number of noble-metal alloys over definite ranges of composition. In the case of Ag-Mg alloys, various studies of the LPS have been carried out using high-resolution transmission electron microscopy and x-ray diffraction methods; see, for example, Refs. 6–10. The LPS's consist of domains, based on a number of subunits with the $L1_2$ structure, bounded by antiphase boundaries, each with a displacement vector $\frac{1}{2}(\mathbf{a}+\mathbf{b})$, occurring periodically along the $\mathbf{c}$ direction, where $\mathbf{a}$, $\mathbf{b}$, and $\mathbf{c}$ are the fundamental translation vectors of the ($L1_2$) cubic unit cell. Although a number of LPS's with different periods occur in the range 20–30 % Mg, we concentrate here on the simplest one observed, namely, the LPS with the $DO_{23}$ structure,[6] whose unit cell dimension along $\mathbf{c}$ is 4 times that of the $L1_2$ unit.

There appears to be no record of previous photoemission studies on $\alpha'$-$Ag_3Mg$ in the literature, and only limited work has been reported on $\beta'$-AgMg. As far as previous experiments on the latter are concerned, Weightman *et al.*[11,12] determined the valence $d$-band width using x-ray photoelectron spectroscopy (XPS), but their principal interest was to examine the influence of the bandwidth on Auger spectra. Dunsworth *et al.*[13] reported a study of the de Haas–van Alphen effect and they carried out a non-self-consistent nonrelativistic band-structure calculation using the linearized muffin-tin orbital (LMTO) method that produced a Fermi surface in good agreement with their experimental measurements. More recently, Blyth *et al.*[14] calculated the density of states in $\beta'$-AgMg as part of a more general study of the electronic structure in a number of Mg-rich transition metal alloys. However, they did not discuss their results for $\beta'$-AgMg in any quantitative detail. We have also made calculations[15] of the electronic structure in $\beta'$-AgMg using a self-consistent-field (SCF), relativistic, LMTO method within the atomic sphere approximation (ASA) and achieved good agreement between photocurrent calculations and the experimental measurements of Weightman *et al.*[11,12] The only report of previous calculations of the electronic structure in $\alpha'$-$Ag_3Mg$ that we are aware of is by ourselves;[16] we investigated the stability of the LPS structures in Ag-Mg alloys near the 3:1 stoichiometric composition using the SCF-LMTO-ASA method and demonstrated that the $DO_{23}$ structure is more stable than the $L1_2$ and the $DO_{22}$ structures.

In this paper, we report photoemission measurements from $\alpha'$-$Ag_3Mg$, using both uv photoelectron spectroscopy (UPS) and XPS, and further results for $\beta'$-AgMg. We concentrate on measurements of the valence-band spectra and the core-level binding energies for these alloys and the parent metals. We have also carried out

 

electronic structure calculations of $\beta'$-AgMg, with the CsCl structure, and $\alpha'$-$Ag_3Mg$, with both the $L1_2$ and $DO_{23}$ structures, using the SCF-LMTO-ASA method. In order to properly compare the experimental spectra with the electronic structure calculations, we used the self-consistent potentials and densities of states to calculate the photocurrents from the alloys.

## II. EXPERIMENTS

We prepared two polycrystalline specimens containing nominally 50 at.% and 25 at.% Mg. The equiatomic alloy was prepared by remelting the constituents six times in a capped graphite crucible in an argon arc-furnace, followed by an anneal for 10 days at 823 K to ensure homogeneity. There was only a small weight loss during the preparation procedure — assumed to be Mg — and the concentration of the $\beta'$-AgMg sample was determined to be

$$\text{Ag} \rightarrow 49.8 \pm 2 \text{ at.\%}, \quad \text{Mg} \rightarrow 50.2 \pm 2 \text{ at.\%}.$$

The other alloy sample was made similarly, but in order to produce the ordered ($\alpha'$) phase, it was also annealed at 350 °C for 187 h, a temperature just below the published order-disorder transition temperature.[5] The concentration of the $\alpha'$-$Ag_3Mg$ sample was determined to be

$$\text{Ag} \rightarrow 75.9 \pm 2 \text{ at.\%} \quad \text{Mg} \rightarrow 24.1 \pm 2 \text{ at.\%}.$$

The samples were cut into the appropriate size for photoemission measurements by spark-machining and then polished using conventional wet/dry methods to get a smooth surface. Finally, the samples were polished in the standard manner using alumina powder and thoroughly washed in alcohol.

Prior to the photoemission measurements, we carried out a series of electrical resistance measurements on a sample of $Ag_3Mg$ that had been removed from the original boule in order to characterize the order-disorder transition. We found that on heating the transition occurred at $390 \pm 2$ °C, with about a 10 °C hysteresis between the heating and cooling curves. By making time-dependent measurements at a series of fixed temperatures we found that 2 h at 350 °C was certainly sufficient to fully order the sample; the recipe we chose prior to making photoemission measurements. These observations are similar to the previously published data.[5] X-ray diffraction methods were used to determine the ordered structure of the $Ag_3Mg$ sample after the above annealing procedure. We found[17] that the diffraction pattern was very close to that for the $DO_{23}$ structure, as observed by Gangulee and Moss.[6] We also confirmed that the AgMg sample had the CsCl structure. In Table I we list the room temperature lattice constants of the actual samples used for the photoemission measurements and they were obtained by a modified Debye-Scherrer method,[17] based on a design proposed by Gandolfi.[18]

We used angle-resolved Auger electron spectroscopy (AES) to determine and characterize the most suitable surface preparation procedure for the alloys. We found that reproducible and stable surfaces could be produced by $Ar^+$ bombardment at 2 keV and a current of 20 $\mu$A for 30 min, followed by an anneal at 340 °C for $\beta'$-AgMg. The preferred procedure for preparing a $\alpha'$-$Ag_3Mg$ surface following the $Ar^+$ bombardment was to heat the sample to 450 °C for 30 min, cool to 350 °C and hold for 2 h. The composition ratios for both the surface enhanced measurements (i.e., with an emission angle of $\sim 60°$) and the bulk enhanced measurements (i.e., with an emission angle of $\sim 0°$) proved to be very close, indicating little preferential segregation at the surface. The concentrations in the surface region sampled by the measurements were deduced from the peak-to-peak amplitudes of the peaks in the differentiated AES spectra; the composition for the $\beta'$-AgMg sample was $\sim 50 \pm 5$ at.% Mg and for the $\alpha'$-$Ag_3Mg$ sample, it was $\sim 23 \pm 5$ at.% Mg, i.e., the same as the bulk values.

TABLE I. The calculated equilibrium lattice constants, experimental lattice constants at room temperature, and the bulk moduli in ordered Ag-Mg alloys.

| | $\beta'$-AgMg | $\alpha'$-$Ag_3Mg$ |
|---|---|---|
| $a_{calc}$ (Å) | 3.239 | 4.093 |
| $a_{expt}$ (Å) | 3.3125 | 4.1105 |
| Bulk modulus (Mbar) | 0.91 | 1.14 |

The XPS and UPS measurements were made using a VG-BLADES 500 spectrometer with unmonochromatized Al-K$\alpha$ radiation ($h\nu$ = 1486.6 eV) as the x-ray source and He II radiation ($h\nu$ = 40.8 eV) as the uv source. The measurements were carried out at room temperature and at normal emission with the radiation incident at an angle of 42°; the acceptance half-angle of the analyzer is $\sim 2°$. All of the XPS and UPS spectra shown here were recorded at pass energies of 50 eV and 10 eV, respectively, unless otherwise stated. The instrumental resolution was determined to be close to a Gaussian form with a full width at half maximum (FWHM) of 0.95 eV for XPS and 0.3 eV for UPS.[19]

Since the photoionization cross section for $d$ electrons is much larger than that of $s$ or $p$ electrons,[20] the signal from the Mg valence bands ($3s$) is much smaller than that from the Ag $4d$ bands. Thus the photoemission from the valence bands of the alloys is dominated by the contribution from the Ag $4d$ related states; the Mg contribution merely appears as a "background." In Figs. 1 and 2 we show the XPS and UPS valence-band spectra for $\beta'$-AgMg and $\alpha'$-$Ag_3Mg$, where, for the XPS spectra, a polynomial background subtraction routine was used and for the UPS spectra a Shirley-type function[21] was used.

From these data it appears that the energy positions of the bottom edges of the $d$ bands, i.e., at the greatest binding energies, are approximately the same in the alloys and they also line up with the bottom edge of the $d$ band in the pure Ag spectra. Thus the photoemission measurements indicate that it is the position of the top of the $d$ band that is most significantly affected on alloying. It is apparent also that the width of the $d$ band decreases

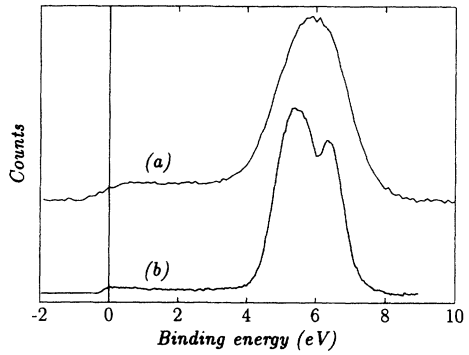


FIG. 1. (a) Photoemission spectrum from $\beta'$-AgMg using Al-K$\alpha$ radiation. (b) Photoemission spectrum from $\beta'$-AgMg using He II radiation.

from pure Ag to $\alpha'$-$Ag_3Mg$ to $\beta'$-AgMg; we will discuss these points in more detail in Sec. IV.

In addition to the valence-band measurements we made measurements of the core-level shifts (CLS's) due to alloying. The binding energy of each core electron in a solid depends on its environment. Since it is to be expected that on alloying some charge redistribution takes place around each site, a CLS is likely to be observed when one compares the XPS peak positions for a particular core level in an alloy with the corresponding core level in the parent metal. Our XPS measurements for the CLS determinations were also made using Al-K$\alpha$ radiation, but to achieve an improved signal to noise ratio, however, we selected a higher pass energy (100 eV) for these measurements. In order to obtain reliable CLS data we ensured that the conditions were the same for the alloy samples and the parent metal samples by referencing their binding energies to those of the 3*d* core levels from a sample of Mo, which was mounted on the sample holder at the same time. This minimizes uncertainties due to the change of sample and instabilities of the analyzer. We carried out measurements of the Ag 3*p*, Ag 3*d*, Ag 4*s*, Mg 2*s*, and Mg 2*p* core levels in pure Ag, pure Mg, $\beta'$-AgMg, and $\alpha'$-$Ag_3Mg$ and the results are listed in Tables II and III.

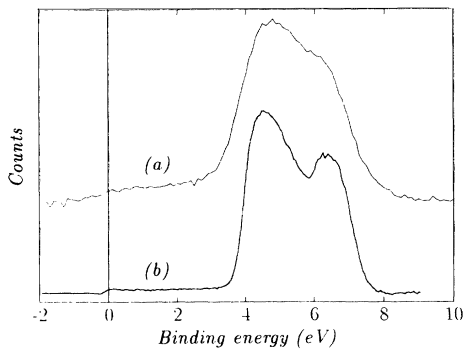


FIG. 2. (a) Photoemission spectrum from $\alpha'$-$Ag_3Mg$ using Al-K$\alpha$ radiation. (b) Photoemission spectrum from $\alpha'$-$Ag_3Mg$ using He II radiation.

TABLE II. Experimental binding energies and core-level shifts for $\beta'$-AgMg.

| Core level | Ag (eV) | $\beta'$-AgMg (eV) | Shift (eV) |
|---|---|---|---|
| Ag $3p^{1/2}$ | 604.02 | 604.50 | 0.48±0.10 |
| $3p^{3/2}$ | 573.22 | 573.65 | 0.43±0.10 |
| $3d^{3/2}$ | 368.17 | 368.70 | 0.53±0.10 |
| $3d^{5/2}$ | 374.17 | 374.70 | 0.53±0.10 |
| $4s^{1/2}$ | 97.12 | 97.45 | 0.33±0.10 |
| **Core level** | **Mg (eV)** | **$\beta'$-AgMg (eV)** | **Shift (eV)** |
| Mg $2s^{1/2}$ | 88.57 | 88.70 | 0.13±0.10 |
| $2p^{1/2}$ | 49.57 | 49.75 | 0.18±0.10 |
| $2p^{3/2}$ | 49.57 | 49.75 | 0.18±0.10 |

## III. CALCULATIONAL DETAILS

We calculated the electronic structures of Ag (fcc structure), $\beta'$-AgMg (CsCl structure) and $\alpha'$-$Ag_3Mg$ ($DO_{23}$ structure with $c/a = 4.0$) using the SCF-LMTO-ASA method.[22,23] The LMTO-ASA method is a fast technique — at the expense of only a small loss in accuracy — and is particularly useful when used for structures with many atoms per unit cell (such as the $DO_{23}$ structure, with 16 atoms/cell). In our calculations we only included angular momentum components up to $\ell = 2$ in the basis functions since we expect that higher components play a negligible role in Ag-Mg alloys. We assumed equal atomic sphere radii for Ag and Mg — in earlier studies of $\beta'$-AgMg (Ref. 15) we found that the use of different sphere sizes had an insignificant effect on results — and we used the von Barth–Hedin form for the local exchange and correlation.[24] When determining initially the equilibrium Wigner-Seitz radii we used the scalar relativistic approximation; in a final set of calculations the core states were treated fully relativistically and were relaxed during the iteration process and the spin-orbit interaction in the valence states was included variationally. Further technical details can be found in Refs. 25 and 26. We carried out the self-consistency cycles on grids of 165 **k** points for $\beta'$-AgMg and 135 **k** points

TABLE III. Experimental binding energies and core-level shifts for $\alpha'$-$Ag_3Mg$.

| Core level | Ag (eV) | $\alpha'$-$Ag_3Mg$ (eV) | Shift (eV) |
|---|---|---|---|
| Ag $3p^{1/2}$ | 604.07 | 604.30 | 0.23±0.10 |
| $3p^{3/2}$ | 573.22 | 573.35 | 0.13±0.10 |
| $3d^{3/2}$ | 368.12 | 368.30 | 0.18±0.10 |
| $3d^{5/2}$ | 374.12 | 374.30 | 0.18±0.10 |
| $4s^{1/2}$ | 97.12 | 97.40 | 0.28±0.10 |
| **Core level** | **Mg (eV)** | **$\alpha'$-$Ag_3Mg$ (eV)** | **Shift (eV)** |
| Mg $2s^{1/2}$ | 88.57 | 89.00 | 0.48±0.10 |
| $2p^{1/2}$ | 49.57 | 50.10 | 0.53±0.10 |
| $2p^{3/2}$ | 49.57 | 50.10 | 0.53±0.10 |

for $\alpha'$-$Ag_3Mg$ in the irreducible wedges of the Brillouin zones. When calculating the density of states (DOS) we increased the number of **k** points in the wedges to 455 for $\beta'$-AgMg and 273 for $\alpha'$-$Ag_3Mg$. (The reason we used a smaller number of **k** points in the latter case is because of the greater number of atoms in the unit cell of the $DO_{23}$ structure compared with the former; the calculation is very time consuming and it is impractical to use a larger number of **k** points. In previous related work[16] we found that 273 **k** points is enough for a reliable result.)

## IV. RESULTS AND DISCUSSION

By investigating the variation of the total energies and the pressures with volume we obtained values of the equilibrium lattice constants and the bulk moduli for each alloy. The results are shown also in Table I together with the corresponding experimentally measured values of the lattice constants. We note that the calculated lattice constants are all smaller than the experimental values. One explanation is that the LMTO calculation represents 0 K whereas the experimental results are the room temperature values (25 °C). In addition, such discrepancies are typical for transition metals and alloys using a calculational scheme involving the local density and atomic sphere approximations since, in general, these approximations appear to overemphasize the bonding.

In Figs. 3–5, we show the calculated DOS for pure Ag, $\beta'$-AgMg, and $\alpha'$-$Ag_3Mg$. These curves clearly show that the valence-band region of the alloys is dominated by the Ag 4*d* related states and that the amount of Mg *s*-*p* hybridization is relatively small. The DOS of the alloys are narrower than that for pure Ag; the *d*-band width in the alloy depends on the number of Ag-Ag nearest neighbor bonds and the distance between the two atoms in that bond. A decrease in the number of Ag-Ag nearest neighbor bonds and/or an increase in the bond length will decrease the *d*-band width because of the reduced overlap of the Ag 4*d* wave functions. In Ag there are 12 Ag-Ag bonds and the distance between the atoms is $a_0/\sqrt{2}$, where $a_0$ is the lattice spacing of the cubic unit cell. In $\beta'$-AgMg, the number of nearest neighbor Ag-Ag bonds is 6 and the Ag-Ag distance is $a_0$, which is some 12% greater than that in pure Ag. As a result the *d*-band width in this alloy is much smaller than that in pure Ag. In $\alpha'$-$Ag_3Mg$, since the ordered structure is based on $L1_2$ structure, the number of Ag-Ag nearest neighbor bonds is 8 and the Ag-Ag distance is $a_0/\sqrt{2}$. Therefore there will be a reduction in the Ag 4*d* band width in $\alpha'$-$Ag_3Mg$ also, but it will not be reduced as much as in the case of $\beta'$-AgMg.

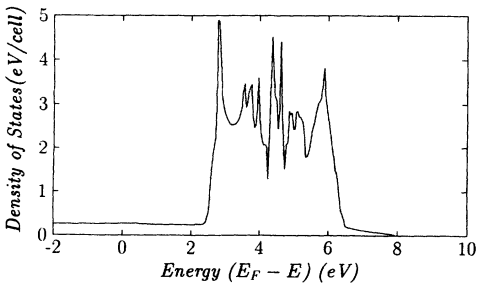


FIG. 3. The total density of states for Ag calculated using the SCF-LMTO-ASA method.

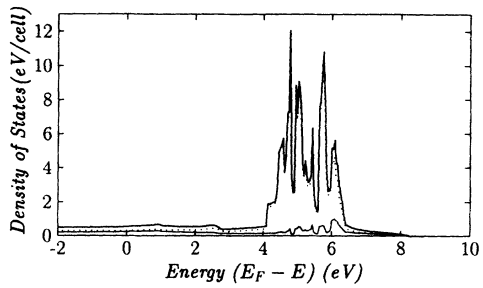


FIG. 4. The total and site decomposed densities of states of $\beta'$-AgMg calculated using the SCF-LMTO-ASA method. The points are for the Ag site, the thinner line is for the Mg site, and the thicker line is the total density of states.

It has been shown (see below) that there is a strong connection between XPS measurements and the density of states. If we compare the UPS and XPS spectra for $\beta'$-AgMg and $\alpha'$-$Ag_3Mg$ with the DOS shown in Figs. 4 and 5, we can see that most of the features in the DOS are reproduced in the experimental spectra, i.e., the narrowing of the *d*-band width resulting predominantly from a shift in energy of the upper *d*-band edge while the position of the lower band edge remains roughly the same. However, such direct comparisons between DOS and the experimental spectra ignore the possible effects of the photon-electron matrix elements, etc. Therefore, it is more realistic to compare the experimental spectra with the calculated electronic structures through appropriate photocurrent calculations.

According to Winter *et al.*[27] the photocurrent is closely related to the density of states, viz.,

$$I(E+\omega) \propto \sum_{\alpha,\ell} |M^{\alpha}_{\ell'\ell}(\omega, E)|^2 n_{\alpha,\ell}(E)\,,$$

where $n_{\alpha,\ell}(E)$ is the local density of states at energy $E$ for angular momentum $\ell$ and atom type $\alpha$, $M^{\alpha}_{\ell'\ell}(E,\omega)$ is the electron-photon matrix element linking the initial

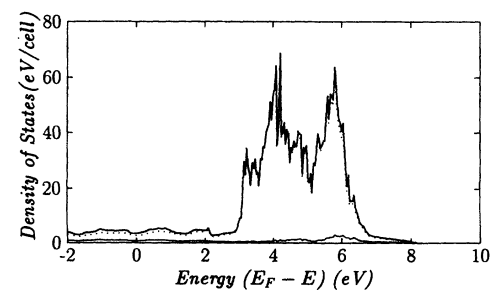


FIG. 5. The total and site decomposed densities of states of $\alpha'$-$Ag_3Mg$ ($DO_{23}$ structure) calculated using the SCF-LMTO-ASA method. The points are for the Ag site, the thinner line is for the Mg site, and the thicker line is the total density of states.

and final states (with $\ell' = \ell \pm 1$), and $\omega$ is the photon energy. Winter *et al.*[27] developed this approach into a calculational scheme for the photocurrent in which one can also include the effects of the hole lifetime. We do not know the lifetimes that occur in the photoemission measurements on Ag-Mg alloys; we used an expression for the inverse lifetime of the form

$$\Gamma = A|E - E_F|^{\frac{1}{2}} \quad (1)$$

in the calculation, where $A$ (= 0.218 eV) was chosen to provide reasonable agreement with experiment in the case of UPS from $\beta'$-AgMg. We used the potentials and DOS from our LMTO calculations as input in the photocurrent calculations and we included a Gaussian broadening function with a suitable value of the FWHM to represent the experimental resolution.

In Figs. 6 and 7 we show the results of our UPS and XPS photocurrent calculations for the two alloy samples. (We acknowledge that, because of the single scatterer approximation used in the theory of Winter *et al.*,[27] the calculations can be unreliable at low photon energies but our experience is that they are realistic above $\sim$ 40 eV.) Comparing these spectra in turn with the experimental results we find that the shapes and widths are very similar, implying that lifetime effects do not play a major role in determining the shape and width of the spectra. However, the peak positions in the calculated photocurrents are $\sim$ 0.6 eV closer to the Fermi energy than those measured experimentally; similar shifts have been observed in the case of other ordered noble metal alloys.[28–30] Presumably, the discrepancy results from the use of the local density approximation and our neglect of the real part of the self-energy[31] that occurs in the photoemission process. The largest difference between the calculated photocurrent and the experimental spectra occurs for UPS from $\alpha'$-$Ag_3Mg$; compare Figs. 2(b) and 7(b). The DOS has some structure on the upper $d$-band edge that is apparent in the calculated photocurrent but does not seem to appear in UPS. (A calculation of the DOS for $Ag_3Mg$ with the $L1_2$ structure also shows similar structure and so it is not an artifact of the $DO_{23}$ calculation.) It is not clear to us why there is this difference although it could be related to our choice of a "simple" Lorentzian broadening function to mimic the effect of the hole lifetime and/or the assumed variation of the latter [i.e., Eq. (1)].

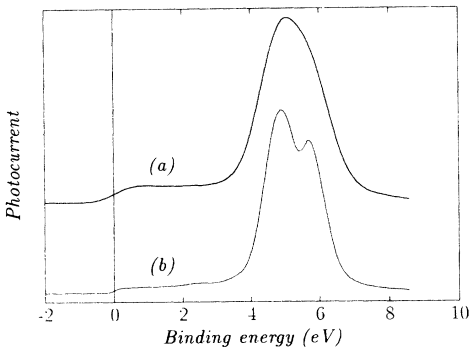


FIG. 6. The calculated photocurrent for $\beta'$-AgMg with (a) $h\nu = 1486.6$ eV (i.e., Al-K$\alpha$ radiation) and (b) $h\nu = 40.8$ eV (i.e., He II radiation), using the densities of states and self-consistent potential functions from a SCF-LMTO-ASA calculation.

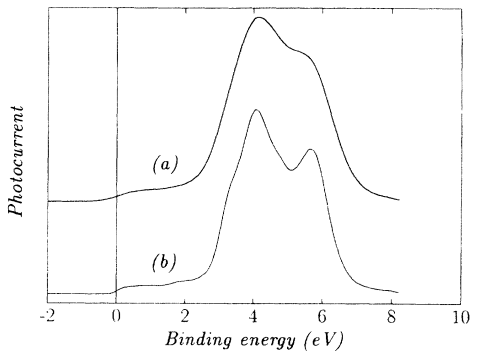


FIG. 7. The calculated photocurrent for $\alpha'$-$Ag_3Mg$ ($DO_{23}$ structure) with (a) $h\nu = 1486.6$ eV (i.e., Al-K$\alpha$ radiation) and (b) $h\nu = 40.8$ eV (i.e., He II radiation), using the densities of states and self-consistent potential functions from a SCF-LMTO-ASA calculation.

In Figs. 8 and 9 we show the Fermi surfaces of $\beta'$-AgMg and $Ag_3Mg$ (with the $L1_2$ structure) in the unfolded Brillouin zone wedges. The topology in the case of $\beta'$-AgMg is very similar to that calculated by Dunsworth *et al.*[13] and is in very good agreement with their experimental results. The topology of the Fermi surface in $Ag_3Mg$ has a number of interesting features.[16] There are three bands that cross the Fermi energy and for clarity we have shown them individually in Fig. 9. The surface from the lowest band, Fig. 9(a), is very similar to that obtained within the empty lattice approximation with an $e/a$ ratio of 5/4. The surfaces generated by the two other bands show substantial deviations from free-electron-like behavior. Recently, we argued[16] that the formation of the LPS structures observed in alloys near the 3:1 stoichiometric composition — of which the $DO_{23}$ structure is the simplest example — is driven by topological features of the surface generated by the uppermost band. It can be seen in Fig. 9(c) that at the 3:1 composition this surface has straight regions (labeled $\mathbf{a} - \mathbf{a}'$) parallel to $MX$ at a distance of almost exactly $0.75|\Gamma X|$ from $MX$. The argument is that the formation of the $DO_{23}$ structure will produce a superzone boundary at this position; thus a gap appears at the Fermi energy with a concomitant lowering of the electronic energy that stabilizes the LPS

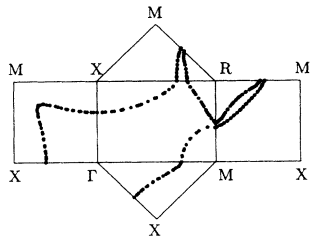


FIG. 8. The Fermi surface of $\beta'$-AgMg in the unfolded irreducible wedge of the Brillouin zone.

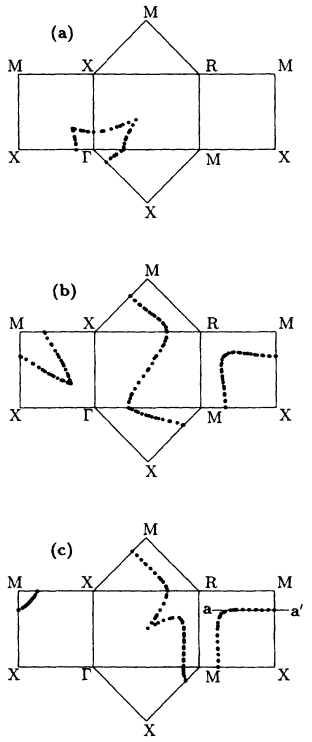


FIG. 9. The Fermi surface of $Ag_3Mg$ ($L1_2$ structure) (a) for band 17, (b) for band 18, and (c) for band 19.

structure.[16] We also showed that such an argument would account for the observed variation in the modulation of the LPS structures with composition.

The results of the CLS measurements displayed in Tables II and III also show some interesting behavior. We note that the values of the Ag and Mg core-level binding energies are in good agreement with the current best values.[32] The results show that in $\beta'$-AgMg, the binding energies of the Ag core levels are $\sim$ 0.5 eV larger than those in pure Ag whereas the binding energies of the Mg core levels are only a slightly larger than those in the pure Mg. In $\alpha'$-$Ag_3Mg$, the Ag CLS are smaller than in $\beta'$-AgMg, but the Mg CLS are larger than in $\beta'$-AgMg. However, we note that in all cases, the Ag and Mg core levels are both shifted to higher binding energies in the alloys. Thus the simple (ground state) view of a "transfer of charge" is wholly inappropriate since it follows that the individual CLS would then be of opposite sign. We believe that relaxation effects are important here and will produce the apparent "change" in the sign of the CLS for Mg compared with that obtained using the eigenvalues from the LMTO calculations. A further discussion on the CLS in Ag-Mg alloys and an attempt to make a realistic first-principles approach that includes relaxation effects will be reported shortly in another paper.[33]

As stated earlier, the width of the valence $d$ bands depends on the number of the nearest neighbor Ag-Ag bonds and the distances between the two atoms. The fewer number of bonds and the greater the distance, the smaller the valence bandwidth. We show the variation of

TABLE IV. The $d$-band widths in ordered Ag-Mg alloys from the experimental measurements and the calculations. (The estimated error in the UPS and XPS measurements is $\pm 0.05$ eV.)

| | Ag | $\beta'$-AgMg | $\alpha'$-$Ag_3Mg$ |
|---|---|---|---|
| XPS (eV)[a] | 3.37 | 3.22 | 2.38 |
| UPS (eV)[a] | 3.15 | 3.03 | 2.04 |
| DOS (eV)[b] | 3.81 | 3.66 | 2.98 |

[a]FWHM values.
[b]Measured at the base of the peak; see text.

the $d$ band widths (from the experimental spectra and the DOS) with composition in Table IV. The widths of the experimental spectra are FWHM, and the values from the DOS are measured close to the base of the peaks because of the structure in the DOS, particularly on their uppermost edges; see Figs. 4 and 5. Thus it is not entirely appropriate to compare directly the widths obtained from the DOS calculations with those from UPS and XPS. However, one can see that the measured and calculated widths for Ag, $\beta'$-AgMg, and $\alpha'$-$Ag_3Mg$ show the expected trend.

## V. SUMMARY

In this paper we report an investigation of the electronic structure in two ordered Ag-Mg alloys, namely, $\beta'$-AgMg (with the CsCl structure) and $\alpha'$-$Ag_3Mg$ (with the $DO_{23}$ structure) using a combination of UPS and XPS measurements and first-principles band-structure and photocurrent calculations. Overall, the agreement between the experimental data and the calculations is good, although some small discrepancies appear in the case of comparisons between the experimental and calculated UPS spectra for $\alpha'$-$Ag_3Mg$. We conclude that the one-electron approach provides a realistic description of the valence-band electronic structure in ordered Ag-Mg alloys. We find that the measured Ag and Mg core-level shifts on alloying are in the same direction, suggesting that relaxation effects are important in these alloys.

## ACKNOWLEDGMENTS

This work was supported with funds from the NSF (Grant No. DMR-9120120). R.G.J. is grateful to NATO for travel funds to visit the Daresbury Laboratory, under the Collaborative Research Grants Programme, and he and Y.L. thank Dr. P.J. Durham and Dr. G.Y. Guo of the Theory and Computational Science Division at Daresbury for their help and kind hospitality. The authors are grateful to Florida State University for the provision of CRAY supercomputer resources and Y.L wishes to express her thanks to the Department of Physics, Florida Atlantic University for partial financial support.

[1] R.G. Jordan and P.J. Durham, in *Alloy Phase Stability*, edited by G.M. Stocks and A. Gonis (Kluwer Academic, Dordrecht, 1989), pp. 35–74.
[2] M. Hansen and K. Anderko, *Constitution of Binary Alloys* (McGraw-Hill, New York, 1958).
[3] C. Barrett and T.B. Massalski, *Structure of Metals*, 3rd revised ed. (Pergamon, Oxford, 1980), Chap. 11.
[4] See, for example, K. Girgis, in *Physical Metallurgy, Part 1*, edited by R.W. Cahn and P. Haasen (North-Holland, Amsterdam, 1983), p. 220; T.B. Massalski, *ibid.*, p. 153.
[5] A. Gangulee and M. Bever, Trans. Met. Soc. AIME **242**, 278 (1968).
[6] A. Gangulee and S.C. Moss, J. Appl. Cryst. **1**, 61 (1968).
[7] K. Hanhi, J. Mäki, and P. Paalassalo, Acta Metall. **19**, 15 (1971).
[8] M. Guymont, R. Portier, D. Gratias, and W.M. Stobbs, in *Modulated Structures—1979*, Proceedings of the International Conference on Modulated Structures, AIP Conf. Proc. No. 53, edited by J.M. Cowley, J.B. Cohen, M.B. Salamon, and B.J. Wuensch (American Institute of Physics, New York, 1979), p. 256.
[9] Y. Fujino, H. Sato, and N. Otsuka, in *Materials Problem Solving with the Transmission Electron Microscope*, edited by L.W. Hobbs, K.W. Westmacott, and D.B. Williams, MRS Symposia Proceedings No. 62 (Materials Research Society, Pittsburgh, 1986), p. 349.
[10] J. Kulik, S. Takeda, and D. de Fontaine, Acta Metall. **35**, 1137 (1987).
[11] P. Weightman, P.T. Andrews, and A.C. Parry-Jones, J. Phys. C **12**, 3635 (1979).
[12] P. Weightman and P.T. Andrews, J. Phys. C **13**, 3529 (1980).
[13] A.E. Dunsworth, J.P. Jan, and H.L. Skriver, J. Phys. F **8**, 1427 (1978).
[14] R.I.R. Blyth, P.T. Andrews, N. Heritage, and P.J.R. Birtwistle, J. Phys. Condens. Matter **3**, 8869 (1991).
[15] R.G. Jordan, A.M. Begley, Y. Liu, S.L. Qiu, and R.I.R. Blyth, Solid State Commun. **81**, 667 (1992).
[16] R.G. Jordan, Yan Liu, S.L. Qiu, and Xumou Xu, Phys. Rev. B **47**, 16 521 (1993).
[17] Yan Liu, Ph.D. thesis, Florida Atlantic University, 1993.
[18] G. Gandolfi, Miner. Petrogr. Acta **13**, 67 (1967).
[19] R.G. Jordan, Y. Jiang, M.A. Hoyland, and A.M. Begley, Phys. Rev. B **43**, 12 173 (1991).
[20] J.J. Yeh and I. Lindau, At. Data Nucl. Data Tables **32**, 1 (1985).
[21] D.A. Shirley, Phys. Rev. B **5**, 4709 (1972).
[22] O.K. Andersen, Phys. Rev. B **12**, 3060 (1975).
[23] H.L. Skriver, *The LMTO Method* (Springer-Verlag, Berlin, 1984).
[24] U. von Barth and L. Hedin, J. Phys. C **5**, 1629 (1972).
[25] W.M. Temmerman, P.A. Sterne, G.Y. Guo, and Z. Szotek, Mol. Sim. **4**, 153 (1989).
[26] W.M. Temmerman and P.A. Sterne, J. Phys. Condens. Matter **2**, 5529 (1990).
[27] H. Winter, P.J. Durham, and G.M. Stocks, J. Phys. F **14**, 1047 (1984).
[28] P. Weinberger, A.M. Boring, R.C. Albers, and W.M. Temmerman, Phys. Rev. B **38**, 5357 (1988).
[29] R.G. Jordan, D.M. Zehner, N.M. Harrison, P.J. Durham, and W.M. Temmerman, Z. Phys. B **75**, 291 (1989).
[30] R.G. Jordan, A.M. Begley, Y. Jiang, and M.A. Hoyland, J. Phys. Condens. Matter **3**, 1685 (1991).
[31] G. Wendin, *Breakdown of the One-Electron Pictures in Photoelectron Spectra* (Springer-Verlag, Berlin, 1981), Vol. 45.
[32] J. Kirz, D.T. Attwood, B.L. Henke, M.R. Howells, K.D. Kennedy, K.J. Kim, J.B. Kortright, R.C. Perera, P. Pianetta, J.C. Riordan, J.H. Scofield, G.L. Stradling, A.C. Thompson, J.H. Underwood, D. Vaughan, G.P. Williams, and H. Winick, *Center for X-Ray Optics: X-Ray Data Booklet*, edited by D. Vaughan (Lawrence Berkeley Laboratory, Berkeley, CA, 1986).
[33] R.G. Jordan, Yan Liu, S.L. Qiu, P.J. Durham, and G.Y. Guo (unpublished).